

# Estimation and Validation of Land Surface Temperature (LST) from Landsat 8 OLI and TIRS sensor's Data

Amrit Kamila, Ashis Kr. Paul, Jatisankar Bandyopadhyay

<sup>1</sup>Department of Remote Sensing and GIS, Vidyasagar University, Midnapore-721102, West Bengal, India

<sup>2</sup>Department of Geography & EM, Vidyasagar University, Midnapore-721102, West Bengal, India

Email: [amritkamila90@gmail.com](mailto:amritkamila90@gmail.com)

## Abstract:

*In thermal remote sensing, the emitted radiations from the ground objects are measured for estimating the surface temperature. This measurement is providing the radiant temperature of a body which depends on two factors such as kinetic temperature and emissivity. The Split Window (SW) is a suitable algorithm to estimate the land surface temperature from Landsat 8, TIRS data. In this study NDVI is the chief parameter, which is computed from NIR and RED band of Landsat 8, OLI Sensor's data. The ratio is done after the DOS correction and converting the DN to top of the atmospheric spectral radiance and then reflectance. Then the Land Surface Emissivity (LSE) is estimated through the Fractional Vegetation Coverage (FVC) which is obtained from NDVI. The Split Window (SW) algorithm calculates the Brightness Temperature of band 10 with combining some coefficient and Land Surface Emissivity (LSE) is considered to estimate the Land Surface Temperature (LST) for each ground pixel. After that, some field survey record has been collected to validate this model. The comparative transect study is finalized to validate this model.*

**Keywords:** Normalized Differences Vegetation Index (NDVI), Fractional Vegetation Coverage (FVC), Land Surface Emissivity (LSE), Brightness Temperature (TB), Land Surface Temperature (LST), Split Window (SW) Algorithm.

## 1. Introduction

Thermal remote sensing is the part of remote sensing to facilitate the acquisition, dispensation and explanation of data which is obtained mainly in the thermal infrared (TIR) region of the electromagnetic (EM) spectrum. Thermal infrared remote sensing technology is an imperative method to study the thermal characteristics of the land surface. The Split Window (SW) algorithm occupies two thermal bands which are characteristically located in the atmospheric window between 10 and 12  $\mu\text{m}$  [15]. The foundation of this algorithm is that, the radiance diminution for atmospheric absorption is proportional to the radiance disparity of instantaneous

measurements of two different wavelengths [14]. This technique measures the radiation of a target area which is emitted from the surface; on the other hand the optical remote sensing measures the radiations which are reflected from the target [6]. Most of the energy is sensed by the sensor which is directly emitted from the land surface [4]. The Split Window (SW) algorithm was first proposed by McMillin [10], it is recommended using the differences in the atmospheric absorbance of two adjacent Long wave infrared (LWIR) bands in order to retrieve the Sea Surface Temperature (SST). The LST retrieval method for Landsat 8 has been developed a tool [1] for the complicated process of obtaining the LST from the surface. Landsat 8 is the newest mission (February, 2013) of the Landsat project. Thermal Infrared Sensor (TIRS) of the Landsat 8 provides two adjacent thermal bands (Band 10 and Band 11) to continue the thermal imaging ability of the Landsat program, which has an enormous advantage for the LST inversion. Land Surface Temperature (LST) demonstrates the temperature of the surface, it is measured in Kelvin. Several numbers of algorithms have been premeditated to calculate the Land surface temperature. Thermal infrared (TIR) remote sensing contributes a tremendous method for gaining the LST information at the regional and global scales. The normal field of view (stray light) has affected in TIRS Bands 10 and 11 of Landsat 8 data. Band 11 is significantly more infected by stray light than Band 10. It is recommended that users refrain from using Band 11 data in quantitative analysis including the use of Band 11 in Split window surface temperature retrieval algorithms (Appendix A of the [Landsat 8 Data User Handbook](#)). So, it is the most widely used algorithm for LST retrieval due to the simplicity and robustness.

## 2. Study Area

The study area is located on Gopiballavpur-I and Gopiballavpur-II Block in Paschim Medinipur District, West Bengal, India. The study area lies between 86°41'24"E to 87°02'49" E Longitude and 22° 06'09" N to 22° 19'25" N Latitude (Fig.

1). Basically the study area is composed by the mixed vegetation coverage and agricultural land. The study area is composed basically by the lateritic soil and alluvial soil, the alluvial soil is deposited by the Subarnarekha River. These two blocks are underlined by different geological formations such as hard consolidated rocks of Cenozoic age and unconsolidated alluvium of recent age. Surface topography of this area is very gentle slope from west to east. Temperature begins to rise rapidly from about the beginning of March to April and May is the hottest month of the study area and annual average rainfall of the study area is 1450 to 1500mm.

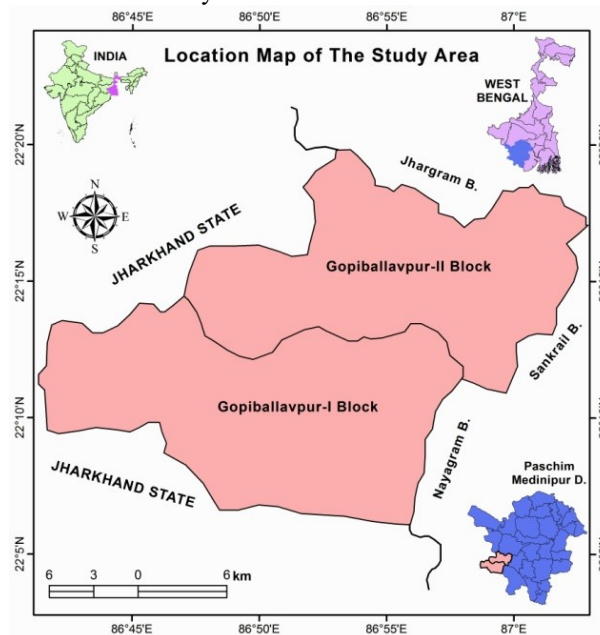


Figure 1. Location of the Study Area

### 3. Data and Methods

Operational Land Imager (OLI) and Thermal Infrared Sensor (TIRS) sensor data of Landsat 8 are compiling by nine spectral bands with a spatial resolution of 30 meters for Bands 1 to 7 and 9. New band 1 (ultra-blue) is useful for coastal and aerosol studies. New band 9 is useful for cirrus cloud detection. The spatial resolution of Band 8 (panchromatic) is 15 meters. Thermal bands 10 and 11 are useful in providing more accurate surface temperatures and are collected at 100 meters. Approximate scene size is 170 km north-south by 183 km east-west (106 mi by 114 mi).

Table 1: Landsat 8 Band Information on 15.03.2017 (Path 139, Row 45)

Landsat 8 Operational Land Imager (OLI) and	Bands	Wave length ( $\mu$ )	Spatial Resolution (m)
	Band 1 -	0.43 -	30

Thermal Infrared Sensor (TIRS)  Imagery Date 15. 03. 2017	Coastal aerosol	0.45	
	Band 2 – Blue	0.45 - 0.51	30
	Band 3 - Green	0.53 - 0.59	30
	Band 4 – Red	0.64 - 0.67	30
	Band 5 - Near Infrared (NIR)	0.85 - 0.88	30
	Band 6 - SWIR 1	1.57 - 1.65	30
	Band 7 - SWIR 2	2.11 - 2.29	30
	Band 8 - Panchromatic	0.50 - 0.68	15
	Band 9 - Cirrus	1.36 - 1.38	30
	Band 10 - Thermal Infrared (TIRS) 1	10.60 - 11.19	100 * (30)
	Band 11 - Thermal Infrared (TIRS) 2	11.50 - 12.51	100 * (30)

TIRS bands are acquired at 100 metre resolution, but these are re-sampled to 30 meters in delivering data product.

Source: Landsat 8 Handbook

Table 2: Metadata of Satellite Imagery

Rescaling factor, Band 10	
$M_L$	0.000342
$A_L$	0.01
Coefficient, Band 10	
$O_i$	0.29
Thermal constant, Band 10	
$K_1$	774.89
$K_2$	1321.08
Emissivity values, Band 10	
$E_v$	0.987
$E_s$	0.971

Source: Landsat 8 Handbook

In this study several band algorithms have been used to Split Window (SW) algorithm for estimating the land surface temperature through the Landsat 8 TIRS bands. Some parameters have been realistically modified in this study to matching the result in this particular region. The band information shows in table (Table 1& Table 2). Methodological flow chart of this study is given below (Fig. 2).

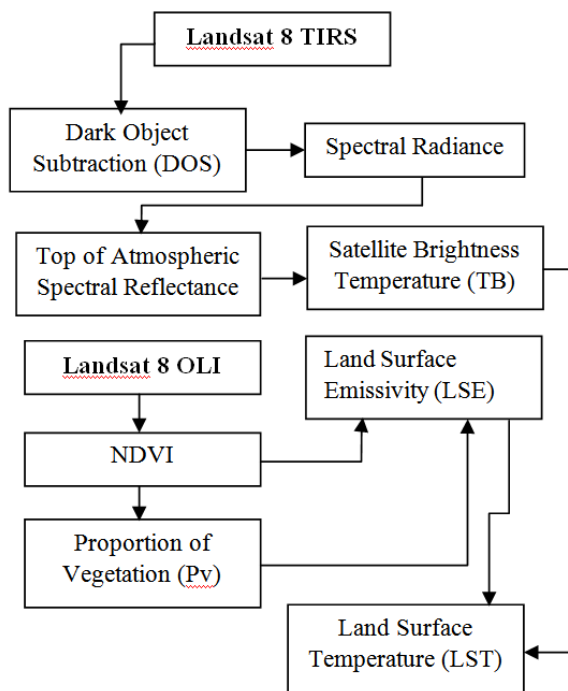


Figure 2. Methodological Flow Chart

### 3.1 Dark Object Subtraction (DOS)

The scattering of the atmosphere, especially depends on the wavelength in the visible part of the electromagnetic spectrum, so the scattering values are particularly correlated with each other. In this context dark object subtraction (DOS) method is accepted because it is a relative atmospheric scattering model to forecast the haze values for all the spectral bands from a selected starting band haze value. This sophisticated method is used to normalize the predicted haze values for the different gain and offset parameters used by the imaging system. It is realistic to use image based techniques for the calculation of these parameters without in situ measurement during image acquisition. The path radiance is given by the following equation [14].

$$L_p = L_{min} - L_{DO1\%} \dots \dots (1)$$

Where,

$L_{min}$ = radiance that corresponds to a digital count value for which the sum of all the pixels with digital counts lower or equal to this value; it is equal to the 0.01% of all the pixels from the image considered [15], therefore the radiance obtained with that digital count value ( $DN_{min}$ );  $L_{DO1\%}$ , radiance of Dark Object, assumed to have a reflectance value of 0.01. Therefore the formula is converted in below:

$$L_{min} = M_L * DN_{min} + A_L \dots \dots (2)$$

The radiance of Dark Object is [15]:

$$L_{DO1\%} = 0.01 * [(ESUN_{\lambda} * \cos\theta_s * T_z) + E_{down}] * T_v / (\pi * d^2) \dots \dots (3)$$

Therefore the path radiance is:

$$L_p = M_L * DN_{min} + A_L - 0.01 * [(ESUN_{\lambda} * \cos\theta_s * T_z) + E_{down}] * T_v / (\pi * d^2) \dots \dots (4)$$

There are several DOS techniques (e.g. DOS1, DOS2, DOS3, and DOS4), based on different assumptions about  $T_v$ ,  $T_z$  and  $E_{down}$ . The simplest technique is the DOS1, where the following assumptions are made [11]:

$$T_v = 1, T_z = 1, E_{down} = 0 \dots \dots (5)$$

Therefore the path radiance is:

$$L_p = M_L * DN_{min} + A_L - 0.01 * ESUN_{\lambda} * \cos\theta_s / (\pi * d^2) \dots \dots (6)$$

The resulting land surface reflectance is transformed:

$$P = [\pi * (L_{\lambda} - L_p) * d^2] / (ESUN_{\lambda} * \cos\theta_s) \dots \dots (7)$$

### 3.2 Conversion to Top of Atmospheric Spectral Radiance

Top of Atmospheric (TOA) Spectral Radiance ( $L_{\lambda}$ ) is the Radiance of the sensor's aperture, it is measured in (Watts / (m<sup>2</sup>\*srad\* $\mu$ m)) this unit [16]. Multispectral and thermal band of the OLI sensor's (Landsat 8) data can be converted to TOA spectral radiance for normalizing the data. On the other hand, for measuring the Brightness Temperature (TB) of an area the Top of Atmospheric (TOA) Spectral Radiance ( $L_{\lambda}$ ) is needed and band rescaling factor is provided in the metadata file [16].

$$L_{\lambda} = (M_L * Q_{cal}) + A_L - O_i \dots \dots (8)$$

Where

$L_{\lambda}$ = TOA spectral radiance [Watts/ (m<sup>2</sup>\*srad\* $\mu$ m)],

$M_L$ = Band specific multiplicative rescaling factor, it is shown in table 2 (Radiance Mult Band X, where X is the band number),

$A_L$ = Band-specific additive rescaling factor (Radiance Add Band X, where, X is the band number),

$Q_{cal}$ = Quantized and calibrated standard product pixel values (DN),

$O_i$ = is the correction for Band number 10 [3].

### 3.3 Conversion to Top of Atmospheric Spectral Reflectance

Different multispectral bands of the OLI sensor's can also be converted to TOA planetary reflectance using reflectance rescaling coefficient factor which are supplied from the product metadata file. The following equation is used [16] to convert spectral radiance to TOA reflectance for OLI data.

$$\rho_p = (\pi * L_{\lambda} * d^2) / (ESUN_{\lambda} * \cos\theta_s) \dots \dots (9)$$

Where

$\rho_p$ = Unit less planetary reflectance, which is "the ratio of reflected versus total power of energy" [16],

$L_{\lambda}$ = Spectral radiance at the sensor's aperture (at-satellite radiance),

$d$  = Earth-Sun distance in astronomical units (provided with Landsat 8 metafile, and an excel file is available from USGS website).

$ESUN_{\lambda}$  = Mean solar exo-atmospheric irradiances,  
 $\theta_s$  = Solar zenith angle in degrees, which is equal to  $(\theta_s = 90^\circ - \theta_e)$ , Where  
 $\theta_e$  is the Sun elevation;  $ESUN$  is the  $(\pi * d^2) * \text{Radiance Maximum and Reflectance Maximum}$   
Where, Radiance Maximum and Reflectance Maximum are provided by image metadata.

So, the Landsat 8 images are made available with band specific rescaling factors which allows for the straight conversion from DN to TOA reflectance. On the other hand, the property of the atmosphere (i.e. Disturbance on the reflectance that varies with the wavelength) should be considered in order to calculate the reflectance at the ground. It is described by the land surface reflectance ( $\rho$ ) [11]:

$$\rho = [\pi * (L_{\lambda} - L_p) * d^2] / [T_v * ((ESUN_{\lambda} * \cos \theta_s * T_z) + E_{down})] \dots \dots (10)$$

Where

$L_p$  = the path radiance,

$T_v$  = the atmospheric transmittance in the viewing direction,

$T_z$  = the atmospheric transmittance in the illumination direction,

$E_{down}$  = the down welling diffuse irradiance.

### 3.4 Conversion to at Satellite Brightness Temperature

Brightness Temperature is the radiation of electromagnetic spectrum, which is traveling upward from the top of the Earth's atmosphere. Thermal bands have been used to calculate the TB. TIRS band data can be converted from spectral radiance to brightness temperature [16] using the thermal constants provided in the metadata file:

$$T_B = K_2 / \ln [(K_1 / L_{\lambda}) + 1] \dots \dots (11)$$

Where

$T_B$  = At satellite Brightness Temperature (K),

$L_{\lambda}$  = TOA spectral radiance (Watts/ (m<sup>2</sup>\*srad\* $\mu$ m)),

$K_1$  = Band specific thermal conversion constant it is shown in table 2 ( $K_1$  constant band  $x$ , where  $x$  is the thermal band number) and  $K_2$ , Band specific thermal conversion constant ( $K_2$  constant band  $x$ , where  $x$  is the thermal band number).

### 3.5 Normal Difference Vegetation Index (NDVI)

Generally the visible and near-infrared bands of Landsat products are used for calculating the Normal Difference Vegetation Index (NDVI). NDVI can measure the amount of vegetation present in the study

area and it can be used to assume the absolute vegetation condition.

$$NDVI = (NIR - RED) / (NIR + RED) \dots \dots (12)$$

On the other hand, the proportion of the vegetation (Pv) is highly associated with the NDVI for the emissivity ( $\epsilon$ ) measurement [12].

### 3.6 Proportion of Vegetation (Pv)

The Proportion of Vegetation (Pv) is similar to the fractional coverage of the vegetation on the surface of the earth [2]. It is calculated using the Normalized Difference Vegetation Index (NDVI) from the OLI sensor's data with the rationing of RED and NIR spectral bands. It is suggested that the NDVI value is used for vegetation and soil to concern in global conditions. But NDVI for soil and NDVI for vegetation will depend on the atmospheric conditions [14]. The values of NDVI are oscillated for each pixel of the study area.

$$Pv = (NDVI - NDVI_{min} / NDVI_{max} - NDVI_{min})^2 \dots \dots (13)$$

Where

Pv = Proportion of Vegetation,

NDVI<sub>s</sub> = NDVI reclassified for soil,

NDVI<sub>v</sub> = NDVI reclassified for vegetation.

### 3.7 Land Surface Emissivity (LSE)

The land surface emissivity ( $\epsilon$ ) is very essential for LST measurement. The surface emissivity is dissimilar to oceans that can fluctuate drastically from unity and deviate with vegetation, surface moisture, roughness, and viewing angles [13]. Although a series of instantaneous LST and LSE retrieval methods have been proposed [7]; [8] and [9] and that can prove to be more precise for satellite derived LST. Split Window algorithm develops Proportion of Vegetation (Pv) to estimate Land Surface Emissivity (LSE) and evaluation of Land Surface Emissivity (LSE) is obtained from the following equation:

$$LSE = \epsilon_s * (1 - Pv) + \epsilon_v * Pv \dots \dots (14)$$

Where

$\epsilon_s$  = the Emissivity for soil,

$\epsilon_v$  = the Emissivity for vegetation which is shown in table 3

Pv = the proportion of vegetation.

### 3.8 Land Surface Temperature (LST)

After calculating all the parameters the Land Surface Temperature (LST) is estimated using the following algorithm [3]. This algorithm is implemented using ERDAS Imagine 13 model builder.



$$LST = BT / 1 + w * ((BT / p) * \ln(e)) \dots\dots (15)$$

Where

- BT= At Satellite Brightness Temperature,
- W= Wavelength of Emitted Radiance (11.5µm),
- [P=  $h * c / s (1.438 * 10^{-2} \text{ mk})$ ],
- H= Plank's Constant ( $6.626 * 10^{-34} \text{ Js}$ )
- S= Boltzmann Constant ( $1.38 * 10^{-23} \text{ J /K}$ ),
- C= Velocity of Light ( $2.998 * 10^8 \text{ m / s}$ ),
- P= 14380 and (e) = Land Surface Emissivity.

## 4. Result and Discussion

### 4.1 Conversion to Top of Atmospheric Spectral Radiance

Radiance is the “flux of energy (primarily irradiant or incident energy) per solid angle, leaving a unit surface area in a given direction”, “Radiance is measured at the sensor and somewhat it depended on reflectance” [16]. The Spectral Radiance at the sensor’s aperture ( $L\lambda$ ) is measured in [watts/(meter<sup>2</sup>\*ster\*µm)] this unit.

### 4.2 Conversion to Top of Atmospheric Spectral Reflectance

Reflectance is the insignificant proportion of incident electromagnetic power which is reflected at a crossing point. Reflectance of the surface material is depending on the effectiveness of reflecting radiant energy. The reflectance of an object property totally depends on the physical and chemical condition of the particular material such as moisture, the surface roughness as well as the geometric circumstances and incidence angle of the sunlight.

### 4.3 Normalized Difference Vegetation Index (NDVI)

The Normalized Difference Vegetation Index (NDVI) is the common ratio for measuring the vegetation coverage of the earth’s surface. It is calculated on a per pixel basis as the normalized difference between the red and near infrared bands from an image. NDVI computes the energy from the visible and near infrared region which is reflected by the vegetation. Healthy vegetation extremely absorbs the visible light and reflects a huge portion of the near infrared light. Unhealthy or sparse vegetation reflects more visible light and less near-infrared light. The very low values of NDVI (0.1 and below) communicate the barren areas of rock, sand, or snow (Fig. 3). Moderate values represent shrub and grassland (0.2 to 0.3), while high value indicates the temperate and tropical rainforests (0.6 to 0.8) [5].

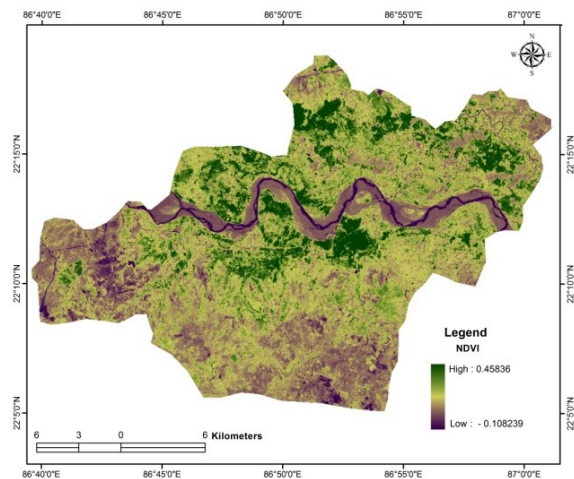


Figure 3. Normalized Difference Vegetation Index (NDVI)

### 4.4 Proportion of Vegetation (PV)

The remoteness between vegetation and soil mechanisms is a significant aspect of this model, because it can relate to the variability at sub-pixel level. So, the fractional vegetation cover is calculated to identify the fraction of the area under vegetation and soil (Fig.4). The Fractional Vegetation Coverage (FVC) would inform us the petite proportion of the total pixels which are enclosed by the trees. Vegetation is the essential component of ecosystem and estimation of fractional vegetation cover is a significant meaning in monitoring the surface emissivity.

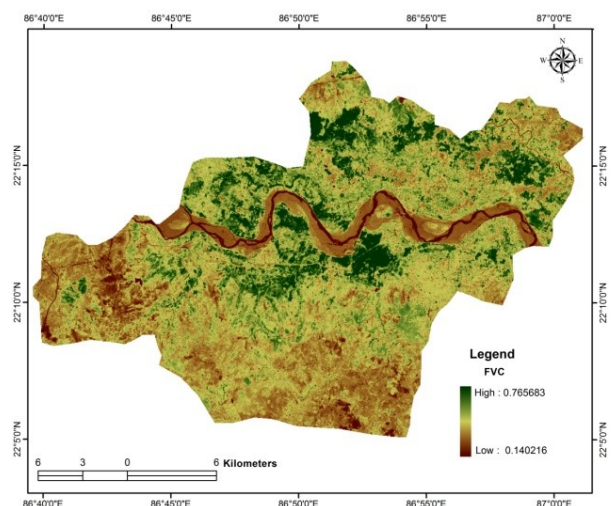


Figure 4. Proportion of Vegetation (PV)

### 4.5 Land Surface Emissivity (LSE)

The measurement of the land surface emissivity is the inherent characteristic of earth’s surface. This method

measures the ability to convert thermal or heat energy into radiant energy. LSE estimation requires for the soil and vegetation of Band 10 because it removes the fraction of radiant energy.

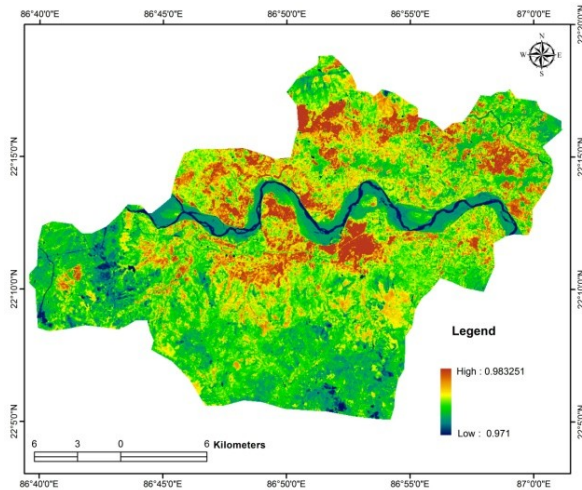


Figure 5. Land Surface Emissivity (LSE)

Emissivity occupies the emitting ability of a real material which is compared to that of a black body and a spectral property that varies with composition of material and the geometric configuration of the surface (Fig. 5). A black body is a theoretical object that absorbs and then emits all incident energy at all wavelengths. This means that the emissivity of such an object is defined by 1. So, the LSE is a proportionality aspect that balances the blackbody radiance (Planck's law) to forecast the emitted radiance.

#### 4.6 Conversion To At Satellite Brightness Temperature (TB)

Brightness Temperature (TB) is the microwave radiance which travels upward from the top of Earth's atmosphere. The calibration method has been made in support of converting thermal DN values of thermal bands to Brightness Temperature (Fig. 6).

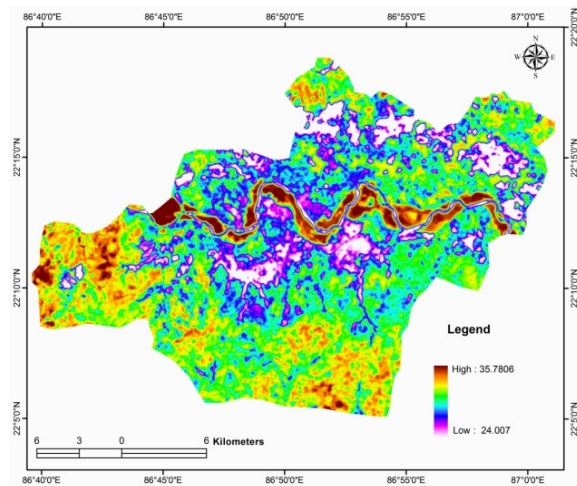


Figure 6. Brightness Temperature

#### 4.7 Land Surface Temperature (LST)

Finally, Land Surface Temperature (LST) is measured from the Landsat 8 TIRS band 10 using Split Window (SW) algorithm that can reflect the surface temperature of the study area. This map shows very high temperature in the sandy areas in the river bed portion (Fig. 7). High temperature occupies the barren type of land in the study area. Fallow land illustrates the moderate temperature. Mixed vegetation and grasslands are screening the low temperature finally thick vegetation and water bodies demonstrate the very low temperature.

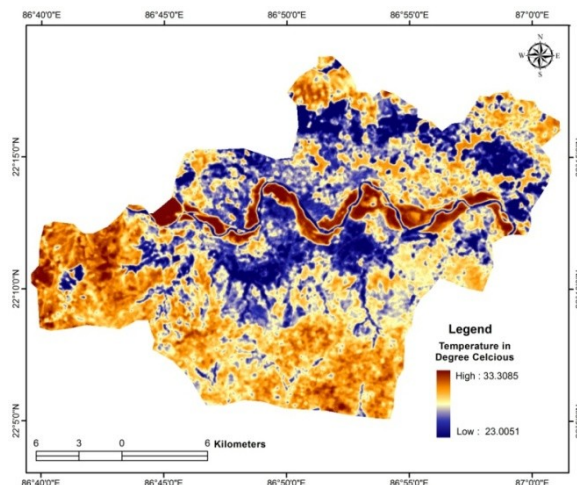


Figure 7. Land Surface Temperature (LST)

#### 4.8 Comparative Study

Types of land use / land cover can play a significant role in nature to control the local climate change. Land Surface Temperature (LST) variability mainly depends on the conversion of land use / land cover due to anthropogenic activities. So, the LST is oscillated in different land use / land cover features. The LST graph is plotted in a composite transect

against the NDVI and Landscape Structure, because NDVI is a replica of land surface features on that area (Fig. 8). This composite transect shows inverse relationships between temperature and land surface features. Where the NDVI value is high the temperature is less, on the opposite way higher temperature denotes the less NDVI value. Because, the positive value of NDVI reflects the green vegetation coverage and the negative value of NDVI focuses the bare soil, dry land and water body. So the presence of green coverage diminishes the temperature, where the NDVI value is high (Fig. 9).

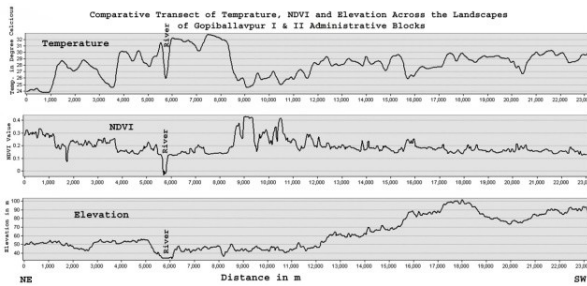


Figure 8. Comparative Transect of Elevation, NDVI and Temperature across the landscapes of Gopiballavpur I & II Administrative Blocks

#### 4.9 Ground Truth Verification (Model Validation)

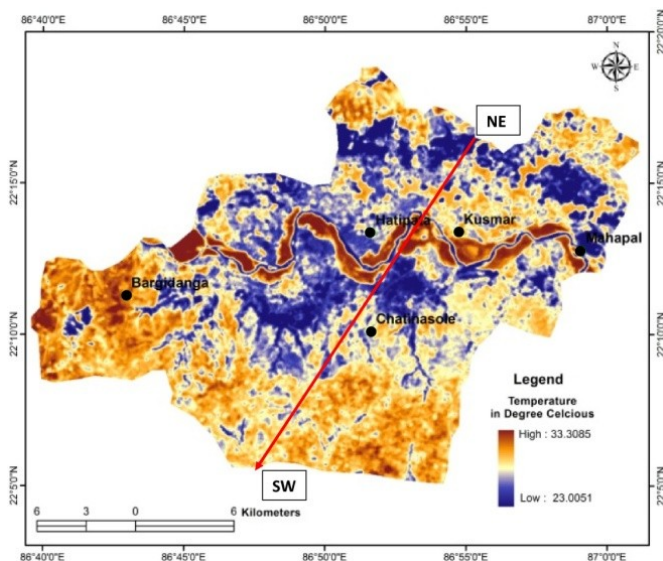
For the model validation, the five stations have been selected on the basis of the field condition where the huge transmission has not been take place for measuring the ground temperature in the entire study area. Station wise on-field temperature data is recorded through the android apps to validate the estimated pixel by pixel land surface temperature from the Landsat 8 TIRS sensor. Three times (9 - 9.30 am, 12.30 - 1 pm and 3.30 - 4 pm) reading of temperature on a particular day at every station has been documented. After averaging the field data it is used for the validation of the ground truth temperature. The station wise field data and the ground location are shown in Table 3 & Fig. 9.

Table 3: Station wise data collected from field on 15.03.2016 (Average temperature of field and surface temperature of satellite image pixel are compared in given sample station)

Station Name	Longitude	Latitude	Field Survey Record			Average Temperature in °C	Pixel Based Temperature in °C
			9.00 - 9.30 AM	12.30- 1.00 PM	3.30- 4.00 PM		
Mahapal	86° 59' 4.630" E	22° 12' 47.176" N	23	30	27	26.66	26.61
Kusmar	86° 54' 44.757" E	22° 13' 23.706" N	22	33	29	28	28.82
Chatinasole	86° 51' 38.466" E	22° 10' 6.190" N	26	31	33	30	29.14
Bargidanga	86° 43' 35.028" E	22° 12' 25.471" N	29	34	33	32	32.13
Hatipata	86° 51' 37.328" E	22° 13' 21.953" N	27	32	33	30.66	29.07

Figure 9. Ground Sample Point and Cross Section Direction

Source: Field survey



#### 5. Conclusions

This study estimates the land surface temperature (LST) through the Split Window (SW) algorithm which is a dynamic mathematical tool for supporting the numerical algorithm to assess the result. The Brightness Temperature (TB) is obtained

from a thermal band of TIRS sensor in Landsat 8. Land Surface Emissivity (LSE) is derived from Fractional Vegetation Coverage (FVC) and Normalized Differences Vegetation Index (NDVI) parameters have been used to evaluate the FVC. Hence the Several coefficients are combined with the above parameters for utilizing the surface temperature. Measuring field survey data and estimated pixel wise imaging data indicate a very close difference of the temperature, this difference illustrates the ± one degree



Celsius error. So, this LST model occupies very small error. The comparative analysis shows the variation of LST is well matched to the land use / land cover types. Therefore the model is very effective, basically for this region.

[16] USGS Handbook, 2013,  
[http://landsat.usgs.gov/Landsat8UsingProduct .php](http://landsat.usgs.gov/Landsat8UsingProduct.php).

## 6. References

- [1] A. Rajeshwari and N. Mani, "Estimation of land surface temperature of dindigul district using landsat 8 data," *International Journal of Research in Engineering and Technology*, vol. 3, no. 5, pp. 122–126, 2014.
- [2] F. Wang, Z. Qin, C. Song, L. Tu, A. Karnieli, and S. Zhao, "An improved mono-window algorithm for land surface temperature retrieval from landsat 8 thermal infrared sensor data," *Remote Sensing*, vol. 7, no. 4, pp. 4268–4289, 2015.
- [3] J.A. Barsi, J.R. Schott, S.J. Hook, N.G. Raqueno, B.L. Markham, and R. G. Radocinski, "Landsat 8 thermal infrared sensor (TIRS) vicarious radiometric calibration," *Remote Sensing*, vol. 6, no. 1, pp. 11607–11626, 2014.
- [4] Jimenez-Munoz, J.C.; Sobrino, J.A. Split-window coefficients for land surface temperature retrieval from low-resolution thermal infrared sensors. *IEEE Geosci. Remote Sens. Lett.* 2008, 5, 806–809.
- [5] John Weier and David Herring (1999), *Measuring Vegetation (NDVI & EVI)*, Earth Observatory, NASA, USA.
- [6] Kahle A.B., 1980. Surface thermal properties. In *Remote Sensing in Geology*, edited by B.S. Siegal, and A.R. Gillespie (New York; John Wiley), pp.257-273
- [7] Li, Z.-L.; Tang, B.-H.; Wu, H.; Ren, H.; Yan, G.; Wan, Z.; Trigo, I.F.; Sobrino, J.A. Satellite-derived land surface temperature: Current status and perspectives. *Remote Sens. Environ.* 2013, 131, 14–37.
- [8] Li, Z.-L.; Wu, H.; Wang, N.; Qiu, S.; Sobrino, J.A.; Wan, Z.; Tang, B.-H.; Yan, G. Land surface emissivity retrieval from satellite data. *Int. J. Remote Sens.* 2012, 34, 3084–3127.
- [9] Masiello, G.; Serio, C.; de Feis, I.; Amoroso, M.; Venafra, S.; Trigo, I.; Watts, P. Kalman filter physical retrieval of surface emissivity and temperature from geostationary infrared radiances. *Atmos. Meas. Tech.* 2013, 6, 3613–3634.
- [10] McMillin L.M. Estimation of Sea Surface Temperatures from Two Infrared Window Measurements with Different Absorption. *J. Geophys. Res.* 1975; 80:5113–5117.
- [11] Moran, M.; Jackson, R.; Slater, P. & Teillet, P. 1992. Evaluation of simplified procedures for retrieval of land surface reflectance factors from satellite sensor output *Remote Sensing of Environment*, 41, 169-184.
- [12] Q. H. Weng, D. S. Lu, and J. Schubring, "Estimation of land surface temperature-vegetation abundance relationship for urban heat island studies," *Remote Sensing of Environment*, vol. 89, no. 4, pp. 467–483, 2004.
- [13] Salisbury, J.W.; D'Aria, D.M. Emissivity of terrestrial materials in the 8–14  $\mu\text{m}$  atmospheric window. *Remote Sens. Environ.* 1992, 42, 83–106.
- [14] Sobrino, J.; Jiménez Munoz, J. C. & Paolini, L. 2004. Land surface temperature retrieval from LANDSAT TM 5 *Remote Sensing of Environment*, Elsevier, 90, 434-440
- [15] Sobrino, J.A.; Caselles, V.; Coll, C. Theoretical split-window algorithms for determining the actual surface temperature. *Il Nuovo Cimento C* 1993, 16, 219–236.